

A kernel integral method to remove biases in estimating trait turnover

Guillaume Latombe^{1*}, Paul Boittiaux¹, Cang Hui^{2,3#}, Melodie McGeoch^{4#}

¹Institute of Ecology and Evolution, The University of Edinburgh, King's Buildings, EH9 3FL, Edinburgh, UK

²Centre for Invasion Biology, Department of Mathematical Sciences, Stellenbosch 7602, South Africa

³Biodiversity Informatics Unit, African Institute for Mathematical Sciences, Cape Town 7945, South Africa

⁴Securing Antarctica's Environmental Future, Department of Environment and Genetics, LaTrobe University, Melbourne 3086, Victoria, Australia

*Corresponding author: glatombe@ed.ac.uk

#These authors share senior authorship

22 Abstract

23

- 24 1. Trait diversity, including trait turnover, that differentiates the roles of species and
25 communities according to their functions, is a fundamental component of biodiversity.
26 Accurately capturing trait diversity is crucial to better understand and predict
27 community assembly, as well as the consequences of global change on community
28 resilience. Existing methods to compute trait turnover have limitations. Trait space
29 approaches based on minimum convex polygons only consider species with extreme
30 trait values. Tree-based approaches using dendrograms consider all species but distort
31 trait distance between species. More recent trait space methods using complex
32 polytopes try to harmonise the advantages of both methods, but their current
33 implementation have mathematical flaws.
- 34 2. We propose a new kernel integral method (KIM) to compute trait turnover, based on
35 the integration of kernel density estimators (KDEs) rather than using polytopes. We
36 explore how this difference and the computational aspects of the KDE computation can
37 influence the estimates of trait turnover. We compare our novel method to existing
38 ones using justified theoretical expectations for a large number of simulations in which
39 we control the number of species and the distribution of their traits. We illustrate the
40 practical application of KIM using plant species introduced to the Pacific Islands of
41 French Polynesia.
- 42 3. Analyses on simulated data show that KIM generates results better aligned with
43 theoretical expectations than other methods and is less sensitive to the total number of
44 species. Analyses for French Polynesia data also show that different methods can lead
45 to different conclusions about trait turnover, and that the choice of method should be
46 carefully considered based on the research question.
- 47 4. Mathematical aspects for computing trait turnover are crucial as they can have
48 important effects on the results and therefore lead to different conclusions. Our novel
49 kernel integral method generates values that better reflect the distribution of species in
50 the trait space than other existing methods. We therefore recommend using KIM in
51 future studies on trait turnover. In contrast, tree-based approaches should be kept for
52 phylogenetic diversity, as phylogenetic trees will then reflect the constrained speciation
53 process.

54

55

56 **Keywords:** Beta diversity, Convex hull, French Polynesia, Trait turnover, Hypervolume,

57 Kernel, Traits

58

59 1. Introduction

60

61 Biodiversity is a complex concept and can most easily be quantified by distinguishing three
62 complementary facets: taxonomic diversity based on a site-by-species matrix that captures
63 the compositional properties of a community; phylogenetic diversity that captures the
64 evolutionary relatedness among community members, using phylogenetic distance between
65 species alongside the site-by-species matrix; and trait diversity that describes a community
66 according to the traits of its residing species, using a species-by-trait matrix alongside the
67 site-by-species matrix (Devictor et al., 2010). The study of functional traits has been
68 advocated as fundamental to better understand and quantify community assembly (McGill
69 et al., 2006), as well as the impact of global change on community resilience and on the
70 ecosystem services that biodiversity provides (Gross et al., 2017). For example, through
71 comparison with null models and by relating traits to environmental gradients and to each
72 other, trait diversity can provide information about the assembly processes structuring an
73 ecological community (Ackerly & Cornwell, 2007), including biotic interactions between
74 species (Laureto et al., 2015). It also enables the estimation of components of ecosystem
75 function, such as nutrient use and storage, or ecosystem productivity (Cadotte et al., 2011;
76 Hillebrand & Matthiessen, 2009).

77

78 In addition to the decomposition of biodiversity into taxonomic, trait and phylogenetic
79 components, unravelling how biodiversity is organised requires an understanding of how
80 assemblages of species are more or less similar to one another at different places and times,
81 i.e. turnover (Anderson et al., 2011). To do so, beta (β) diversity provides a direct link
82 between biodiversity at the regional (gamma – γ – diversity) and local (alpha – α – diversity)
83 scales (Anderson et al., 2011; Chao et al., 2005, 2019). In particular, taxonomic β diversity
84 has been shown to be important for assessing the effects of conservation actions (Socolar et
85 al., 2016), for example for estimating the effect of the spatial distribution of protected areas
86 and their subdivision into multiple subareas on species diversity (Deane et al., 2022), or for
87 extrapolating regional species richness from limited data (Kunin et al., 2018). Although
88 having received less attention than taxonomic β diversity, trait turnover that describes
89 change in trait diversity across communities or regions has also been measured using β

90 diversity for similar applications (e.g. Carmona et al., 2012; Loiseau et al., 2017; Siefert et al.,
91 2013; Swenson et al., 2012; Villéger et al., 2013).

92

93 As a valuable and increasingly measured biodiversity facet, there are multiple important
94 steps to consider when estimating trait turnover over space or time. First, the precise choice
95 of traits can substantially influence the outcome (Petchey & Gaston, 2006). Second, despite
96 recent initiatives to collate large amounts of data for multiple traits across species (e.g.
97 Kattge et al., 2020; Middleton-Welling et al., 2020; Tobias et al., 2022), trait data are still
98 missing for many species and types of traits across taxonomic groups. Finally, and also the
99 focus of this work, different mathematical methods exist to compute trait diversity and
100 turnover that differ in outcome and therefore in the conclusions drawn in biodiversity
101 studies (Loiseau et al., 2017; Sobral et al., 2016; Villéger et al., 2017). A systematic
102 comparison can help identify an informative robust method and establish standards for
103 quantifying trait turnover.

104

105 There are two main categories of methods for calculating trait β diversity: (i) methods based
106 on the concept of trait space (referred to here as the ‘trait space approach’, and (ii)
107 methods that use dendrograms (referred to here as the ‘tree-based approach’). The trait
108 space approach is based on a multi-dimensional space whose axes are determined by the
109 traits included in the analyses. Axes can correspond directly to the original traits or can be
110 derived from these traits through ordinations to reduce dimensionality. A particular species
111 typically represented as a single point in this trait space, and a polytope is computed as the
112 trait envelope of a set of points representing the species of a community or assemblage. The
113 minimum convex polytope (MCP), a convex hull, that encompasses all species of a
114 community in the trait space (Figure 1), has traditionally been used in these analyses
115 (Loiseau et al., 2017). As the MCP only captures information about the species with extreme
116 trait values in a community, it is sensitive to outliers and ignores how species are distributed
117 in the trait space, which can be crucial to delineate the functional roles of different species
118 within an ecosystem (Mouillot et al., 2021). Although other hull methods can be used to
119 compute the trait envelope (e.g. Irl et al., 2017), they are typically computationally intensive
120 and have been seldomly applied to β diversity analyses.

121

122 The tree-based approach consists of computing all pairwise distance between species based
123 on a set of traits, typically using the Gower distance to incorporate both continuous and
124 discrete traits. A clustering algorithm is then applied to these distances to generate a
125 dendrogram, from which measures of β diversity can be computed. Although the tree-based
126 approach considers all species in the computation of trait turnover, the dendrogram splits
127 into successive branches, and using the length of the branches connecting two species as a
128 measure of distance distorts the original trait distance between them compared to the
129 distance obtained through ordination in the trait space. In addition, the choice of the
130 clustering algorithm for generating the dendrogram will inevitably influence the outcome
131 (Loiseau et al., 2017).

132

133 The convex hull of trait space and the tree-based approach therefore make different
134 computational trade-offs, and the appropriateness of the two approaches for measuring
135 trait β diversity has been debated (Loiseau et al., 2017). In response to this debate and to
136 incorporate information from all species, Mammola & Cardoso (2020) proposed another
137 trait space approach where polytopes are defined by applying a threshold to the kernel
138 density estimation (KDE; Figure 1; see details in Methods below). The resulting polytope is
139 typically not convex, and its shape better reflects the distribution of species in the trait
140 space. Although it has the potential to provide a more accurate estimate of trait diversity
141 than the other two methods, this has not been formally assessed. The computational
142 aspects when computing kernel densities have largely been overlooked. These aspects, as
143 we plan to show here, are crucial so that all species contribute to β diversity in the
144 communities.

145

146 Here we propose a new trait space method, which we term the kernel integral method
147 (KIM), for computing trait β diversity based directly on the integration of the KDE rather
148 than on the polytope. We explore how the computational aspects of the KDE computation
149 can influence the estimates of trait β diversity with different methods. For comparison of
150 the existing and new methods, we use a set of theoretical examples for which we can justify
151 how trait β diversity metric should behave. We further apply the KIM method to compute
152 non-native plant trait turnover across islands and archipelagos of the Pacific Islands of
153 French Polynesia and compare results with the other methods.

154

155 2. Methods

156

157 2.1. Trait-space and tree-based approaches

158

159 2.1.1 Convex Hull

160

161 Computing trait turnover between two communities using the convex hull methods simply
162 consists in computing (i) the minimum convex polytopes (MCP) for each community, and (ii)
163 the hypervolumes of the intersection and the union of these two MCPs (Figure 1a,e). It is
164 then possible to compute a range of β diversity indices based on these four values. Here,
165 following Mammola & Cardoso (2020), we used the Jaccard dissimilarity index J (Jaccard,
166 1908) and the Williams replacement index W (Williams, 1996), defined as:

167

$$168 \quad J = 1 - \frac{A \cap B}{A \cup B} \quad \text{Eq.1}$$

$$169 \quad W = \frac{2 \times \min(A - A \cap B, B - A \cap B)}{A \cup B} \quad \text{Eq.2}$$

170

171 where A and B are the hypervolumes of the MCPs for two communities. In our analyses, we
172 computed the MCPs and the indices using the `hull.build()` and `hull.beta()`
173 functions from the BAT R package V.2.8.1 (Cardoso et al., 2015, 2022). The Williams
174 replacement index evaluates the contribution of trait replacement to trait β diversity
175 (Carvalho et al., 2012, 2013), and the difference between Jaccard and Williams indices
176 quantifies how the trait richness difference between communities contributes to β diversity.
177 Although there are other approaches and indices that can decompose β diversity into
178 turnover replacement components, the relevance of these approaches is still debated
179 (Baselga, 2010; Baselga & Leprieur, 2015; Cardoso et al., 2014; Carvalho et al., 2012, 2013).
180 This debate is beyond the scope of this manuscript, and, to compare our methods, we only
181 followed the decomposition used by Mammola & Cardoso's (2020) (see sections on kernel
182 density hypervolumes below), readily available from the BAT R package (Cardoso et al.,
183 2015, 2022).

184

185 The main issue with the convex hull methods is that it is insensitive to the addition or
186 removal of species within the MCP in the trait space (Figure 1). A corollary is that it is
187 sensitive to outliers, as they will define the MCP.

188

189 2.1.2 Tree-based method

190

191 The tree-based method consists in computing a dendrogram from the trait distance
192 between all species in the species pool (i.e. the entire list of species over all included sites,
193 not just those occurring in the pair of sites for each calculation of trait turnover; Figure 2a).
194 Multiple clustering algorithms can be used to generate the dendrogram, but here we
195 followed Loiseau et al. (2017) and used the unweighted pair group method with arithmetic
196 mean (UPGMA) algorithm, using the `hclust()` function from the stats R package (R Core
197 Team, 2022), as it has been shown to best conserve distances between species compared to
198 the original distances in the trait space.

199

200 For each site, a sub-tree including only the species present is generated by trimming the
201 overall tree (Figure 2b,c). It is then possible to compute the trees corresponding to the
202 union and the intersection of the two sub-trees (Figure 2d,e). We can then adapt Eqs 1 and
203 2 to compute the Jaccard and Williams indices, by using the total length of remaining
204 branches. Importantly, the sub-trees must be computed from the original tree generated
205 from the entire species pool, not those computed from only the residing species. This
206 conserves the internal branches in the union and the intersection of the two sub-trees, even
207 if these internal branches do not lead to any present species (see branch h in Figure 2e).
208 Therefore, for the example of Figure 2, Eqs 1 & 2 become:

209

$$210 \quad J = 1 - \frac{A \cap B}{A \cup B} = 1 - \frac{a+b+c+e+h}{a+b+c+e+f+g+h} \quad \text{Eq.3}$$

$$211 \quad W = \frac{2 \times \min(A - A \cap B, B - A \cap B)}{A \cup B} = \frac{2 \times \min(f, g)}{a+b+c+e+f+g+h} \quad \text{Eq.4}$$

212

213 The tree-based method therefore offers the advantage over the convex hull method that all
214 species will be accounted for when computing the β diversity indices. However, the
215 clustering algorithms often generate branch lengths between species in the dendrogram

216 that differ from the original distances in the trait space, which will necessarily influence the
217 value of any β diversity index (Loiseau et al., 2017).

218

219 2.1.3. Kernel density hypervolumes (KDH)

220

221 Mammola & Cardoso (2020) introduced the use of kernel density hypervolumes (KDH) for
222 computing indices of species turnover. This approach uses KDEs to generate polytopes that
223 are often non-convex (and can even be disjoint) and can be seen as a trait envelope around
224 the species points in the trait space. The recommended method is based on a Gaussian
225 estimator of the KDE (Mammola & Cardoso, 2020) and follows a series of four steps (see
226 Blonder et al., 2018 for further details): (i) points are drawn randomly within a hypersphere
227 around each species point in the trait space; (ii) these points are resampled to uniform
228 density; (iii) a KDE is computed from these points; (iv) a threshold (typically 95%) is applied
229 to truncate the KDE and define the polytope, from which hypervolumes can be computed.
230 The indices are then computed as per Eqs 1 & 2. In our analyses, we used the
231 `kernel.beta()` function from the BAT R package V.2.8.1 (Cardoso et al., 2015, 2022) to
232 apply the KDH method.

233

234 This method, although more computationally intensive than the convex hull method, allows
235 to account for the distribution of species points in the trait space to define the polytopes
236 and therefore the hypervolumes used in the computation of the turnover indices (Figure 1b-
237 d,f-h). As a result, the KDH method is less sensitive to outliers.

238

239 The KDH method nonetheless has some caveats. First, the choice of the threshold used to
240 construct the polytope will necessarily influence the components of the β diversity indices,
241 and therefore the final values. Second, by resampling random points to uniform density,
242 some information about the distribution of species points in the trait space is lost. Finally, in
243 the current implementation of the method in the BAT R package V.2.8.1 (Cardoso et al.,
244 2015, 2022), the radius of the hyperspheres within which random points are drawn around
245 the species points and the bandwidth used during the computation of the KDE (the
246 bandwidth is a parameter that determines how smooth the KDE will be) are determined
247 based on the species point distribution of each community separately using the

248 `estimate_bandwidth()` function from the hypervolume R package. As a result, the
 249 more similar species are to each other, the closer random points will be to each other and
 250 the KDE will show a steeper gradient (Figures A1-A24, see especially Figures A1, A9 and
 251 A17). In other words, using different bandwidths and resampling random points to uniform
 252 density gives different weights to a species depending on how different its traits are from
 253 those of other species in the community. For a β diversity index to be unbiased we argue
 254 that all species should have the same weight when relative abundance and intraspecific trait
 255 variation are not concerned.

256

257 2.2 A kernel integral method (KIM)

258

259 Here we propose a novel computational method to compute trait turnover in the trait
 260 space, to solve the issues associated with the KDH method. Our method computes β
 261 diversity indices from the kernels themselves, therefore removing the influence of the
 262 threshold used to generate the polytope, and uses different kernels than those used in the
 263 KDH method. The KIM method consists of using only steps (i) and (iii) from the KDH method:
 264 (i) points (typically 1000, but the number can be adjusted to account for species abundance,
 265 for example) are drawn randomly within a hypersphere around each species point in the
 266 trait space (the diameter of the hypersphere can be the same for all species, or reflect
 267 intraspecific trait variability); (iii) a KDE is computed from these points, and rescaled
 268 between [0,1]. From the KDE, we then propose the following equations to compute the
 269 Jaccard dissimilarity index and the Williams replacement index:

270

$$271 \quad J = 1 - \frac{\int \min(KDE_A, KDE_B)}{\int \max(KDE_A, KDE_B)} \quad \text{Eq.5}$$

$$272 \quad W = \frac{2 \times \min(\int KDE_A - \int \min(KDE_A, KDE_B), \int KDE_B - \int \min(KDE_A, KDE_B))}{\int \max(KDE_A, KDE_B)} \quad \text{Eq.6}$$

273

274 where KDE_A and KDE_B are the KDEs for communities A and B, and $\int KDE_A$ is the integral of the
 275 KDE for community A over all dimensions of the trait space. This is similar in essence to the
 276 index of niche overlap proposed by Mouillot et al. (2005). In practice, since KDEs are
 277 computed as multi-dimensional matrices, an integral is simply computed as the sum of all

278 elements of the matrix. The minimum and the maximum of two KDEs are analogue to the
279 intersection and the union of the polytope in the KDH method (Figure 3).

280

281 This kernel integral method enables us to overcome the limitations of the KDH method
282 mentioned above. First, there is no need to define a threshold: if the KDE is estimated over a
283 large enough area or volume, the local kernel density will approach zero and the integral
284 will therefore converge. Second, the radius within which the random points are drawn is the
285 same for all communities (but a suitable value must be chosen, which can be adjusted to
286 account for intraspecific trait variability). Finally, because there is no resampling to uniform
287 density, the distribution of species points in the trait space will be reflected more accurately
288 in the KDE.

289

290 2.3. Test of the different methods on theoretical data and expectations

291

292 We have described above the theoretical advantages and caveats of each of the different
293 methods. We implemented seven different methods in total to explore how the differences
294 between the characteristics of the methods can influence the results (Table 1):

- 295 • A convex hull method (hereafter COVHULL).
- 296 • A tree-based method (hereafter TREE).
- 297 • The original kernel density hypervolume method with community-specific
298 bandwidths and uniform resampling (hereafter KDH V1).
- 299 • A modified kernel density hypervolume method computed with the same bandwidth
300 for each pair of communities and uniform resampling (hereafter KDH V2), to explore
301 the influence of the bandwidth on the outcome.
- 302 • A kernel integral method using kernel densities estimated with community-specific
303 bandwidths and uniform resampling (hereafter KIM V1), to explore the influence of
304 the kernel-based vs the polytope-based formulas (Figure 3).
- 305 • A kernel integral method using kernel densities estimated with the same bandwidth
306 for both communities within a pair and uniform resampling (hereafter KIM V2), to
307 further explore the influence of the kernel-based vs the polytope-based formulas.

- 308 • A kernel integral method estimated with the same bandwidth for both communities
309 within a pair and without uniform resampling (hereafter KIM V3).

310

311 For each method, we computed Jaccard dissimilarity and Williams replacement, as defined
312 in Eqs 1-6. We then examined how these seven methods behaved in a set of theoretical
313 contexts for which we can make predictions of how an index of turnover should behave to
314 capture trait differences between communities.

315

316 In total, we simulated 72 different pairs of communities (Figures 4 and A1) and computed
317 our 14 indices (the Jaccard and Williams indices for each of the seven methods) for each
318 pair. For simplicity and computational efficiency, we used a trait space defined by two
319 theoretical traits. Each community was first delimited by a MCP represented by four species
320 arranged as a square. The MCPs were either of different sizes (square side of lengths 4 and
321 2; Figure 4) or of the same size (square side of length 4; Figure A1). They were either nested
322 within each other, partially overlapping, or disjunct. For each of these configurations, we
323 generated a community by randomly drawing species points within the MCPs according to
324 three patterns: (i) the species points were located in a small area (square sides of length 1)
325 in opposite corners of the MCPs (hereafter called the “different” point distribution); (ii) the
326 species points were randomly drawn within the MCPs (hereafter called the “random” point
327 distribution); (iii) the species points were located in a small area (squares of length 1) in the
328 closest corners of the MCPs (hereafter called the “similar” point distribution). We tested
329 these 18 configurations for 10, 40, 70 and 100 species points, and performed analyses 50
330 times for each of the resulting 72 configurations (2 MCP size setups x 3 relative positions x 3
331 random point distributions x 4 sets of point numbers x 50 repeats = 72 configurations x 50
332 repeats).

333

334 There is one obvious difference between these theoretical communities and communities
335 that would be analysed for real-world applications: real-world communities belonging to the
336 same ecological system such as those described in the next section will usually share
337 species, resulting in many species points overlapping in the trait space. Here we used
338 independent random species distributions in the trait space for the two communities in
339 order to have more flexibility in these species distributions, to explore in detail how each of

340 the seven methods would behave across a wide variety of extreme configurations, and
341 better test disentangle the implications of their computational specificities.

342

343 This flexibility allows us to describe how a β diversity index should behave based on what it
344 is supposed to capture from these theoretical configurations. These expectations are
345 depicted in Figures 5, A2, A3, and their justification provided in Table A1. In summary,
346 Jaccard dissimilarity should increase as most species points in the two communities move
347 away from each other. The replacement component should decrease if the difference in
348 area covered by the two sets of species points increases. These patterns should be
349 especially clear for large numbers of species, i.e. for high densities of species points. For few
350 species and low species point density (e.g. when only 10 species points were randomly
351 drawn in the trait space), we expect these patterns to be weak, as the stochastic element of
352 the species point distributions may obscure the results.

353

354 2.4. Established non-native plants in French Polynesia

355

356 To examine how the different methods may lead to different conclusions when analysing
357 real data, we examined the trait diversity of plant species introduced to the Pacific islands of
358 French Polynesia, comparing trait turnover across islands and archipelagos using each
359 method. We extracted data from Paciflora (Wohlwend et al., 2021). For French Polynesia,
360 Paciflora contains data on naturalised non-native plant species across the 80 Pacific islands
361 over five archipelagos: The Society Islands, the Gambier Islands, the Tuamotu Islands, the
362 Tubuai Islands, and the Marquesas. However, careful examination of the database revealed
363 that some species were not naturalised but cultivated or endemic. We therefore only used
364 the 417 naturalised species in Paciflora appearing in the Appendix of Fourdrigniez & Meyer
365 (2008).

366

367 For these 417 species, data on species woodiness (woody vs. herbaceous species), seed
368 mass, plant height and specific leaf area (SLA) were extracted from multiple trait databases,
369 including TRY (Kattge et al., 2011, 2020), LEDA (Kleyer et al., 2008), PLANTATT (Hill et al.,
370 2004), Austraits (Falster et al., 2021), BIEN (Maitner, 2022), EcoFlora (Fitter & Peat, 1994),
371 and BROT (Tavşanoğlu & Pausas, 2018). Seed mass, plant height and SLA have been used to

372 characterise different plant life strategies (Díaz et al., 2016; Westoby, 1998). When different
373 databases contained different values, we used the mean for seed mass, plant height and
374 SLA, and the most frequent category for woodiness. Data on plant woodiness was available
375 for all 417 species. Trait data for seed mass and plant height were only available for 250 out
376 of the 417 species. Data for seed mass, plant height and SLA were only available for 124 out
377 of 417 species. We therefore performed three sets of analyses: (i) a set for the 250 species
378 with data on seed mass and plant height, (ii) a set for the 124 species with data on the three
379 traits, and (iii) a set for the same 124 species, using data on seed mass and plant height only,
380 to assess the robustness of the results to data availability and trait selection. In the
381 following we present and discuss mainly results for seed mass and plant height for the 250
382 species (see Figure D1 for the distribution of plant species in this two-dimensional trait
383 space), as it represents more than half of the species and should be less biased despite using
384 only two traits.

385

386 Prior to analysis, seed mass, plant height and SLA were log-transformed and rescaled
387 between [0,1], so that the traits would be more uniformly distributed in the trait space. We
388 then computed the Jaccard dissimilarity and the Williams replacement indices for all species
389 together, and for woody and herbaceous species separately, to have a more comprehensive
390 assessment of potential differences between methods, as woody and herbaceous plants
391 tend to characterise different parts of the global spectrum of plant forms and functions
392 (Díaz et al., 2016). We also computed these indices for all French Polynesian islands, and for
393 each archipelago separately.

394

395 Finally, the behaviours of the different indices were analysed using randomisation tests. We
396 randomised the presence-absence matrices for all islands and for each archipelago by
397 keeping species occupancy and island richness constant (i.e. the sim9 algorithm from
398 (Gotelli, 2000)), and compared the Jaccard dissimilarity and Williams replacement indices
399 generated by the 7 methods for the original matrices to the indices computed over 10
400 randomised matrices for each original matrix (the number of randomisations was
401 constrained by computation time).

402

403 The purpose of these analyses on real data was only to examine how results may differ
404 between methods for more complex data than used in the theoretical analyses, to assess
405 each method's range of sensitivity. As each archipelago contains multiple different islands
406 whose combinations will fall across a large spectrum of trait profile configurations, it was
407 not possible to define a priori expectations and the purpose is therefore not to determine
408 which methods are in line or not with a priori expectations, contrary to the theoretical
409 analyses.

410

411 3. Results

412

413 3.1. Theoretical data

414

415 Overall, KDH and KIM tended to converge towards similar values and behaviours as the
416 number of species points increased (Figures 6-8, C1-C12), corresponding to theoretical
417 expectations (Figures 5, A2, A3). In contrast, the convex hull and the tree-based methods
418 generated indices of turnover different from the other methods and from the theoretical
419 expectations. The main differences between observed and expected values for all methods,
420 except the tree-based method, were for the contribution of replacement to overall turnover
421 (computed as the ratio of the Williams replacement index to the Jaccard dissimilarity index)
422 for MCPs of the same size in the nested / random and the nested / similar configurations,
423 which was lower than the expected value of 1 (Figures A3, C6). This is likely due to the fact
424 these are the configurations for which the values of the Jaccard index are small, and small
425 changes in Williams replacement index due to stochasticity in the distribution of species
426 points in the trait space will be disproportionately large.

427

428 For all indices of turnover, the three KIM methods generated values above 0.5 and above
429 other methods when the point distributions were different from each other (i.e. the
430 "Different" point distributions under all MCP configurations, and for all three point
431 distributions under the "Disjunct" MCP configuration). KIM V3 generated values below 0.5
432 and below other methods when the point distributions were similar from each other (i.e.
433 the "Similar" point distributions under all MCP configurations), and intermediate values

434 otherwise, in-between the values generated by the other methods. These results suggest
435 KIM V3 can better distinguish between different species point distributions in the trait space
436 (Figures 6-8, C1-C12). The KIM V3 method also tended to be less sensitive to the number of
437 species points than the other KDH and KIM methods, with values and behaviours being
438 similar from 10 to 100 species points.

439

440 When communities had MCPs of the same size, the KIM V1 and V2 methods generated
441 similar results to the KDH V1 and V2 methods, respectively, for all β diversity indices
442 (Figures C4-C6, C10-C12). However, when the MCPs had different sizes, the KIM methods
443 tended to generate values more similar to each other than to the KDH methods (Figures 6-8,
444 C1-C3, C7-C8).

445

446 Adjusting the bandwidth to be common between communities in each pair in the
447 computation of the kernels for the KDH and KIM methods (i.e. switching from V1 to V2)
448 resulted in lower dissimilarity values, both for the Jaccard dissimilarity index and the
449 Williams replacement index, for all configurations. This is because the radius of the
450 hyperspheres and therefore the steepness of the kernels were the same for both
451 communities in the V2 methods, increasing similarity. The effect of removing the resampling
452 of random points to uniform density (i.e. from KIM V2 to KIM V3) had an often larger and
453 more variable effect than adjusting the bandwidth, as the values generated by KIM V3 could
454 be either larger, smaller or in between those of the KIM V1 and V2 methods.

455

456 3.2. Established non-native plants in French Polynesia

457

458 Raw values of Jaccard dissimilarity, of Williams replacement and of the contribution of
459 replacement to turnover differed greatly between the different methods. Maximum
460 differences in values between methods were around 0.6 for Jaccard dissimilarity, 0.2 for
461 Williams replacement, and 0.8 for the contribution of replacement to turnover (Figures 9,
462 C2, C3). The KIM V3 and the KDH V2 methods generated the lowest Jaccard dissimilarity,
463 and KIM V1 and TREE the highest. In contrast, KIM V3 consistently generated much higher
464 values for the contribution of replacement to turnover than other methods, as expected
465 from the fact that it better accounts for differences in species point distributions in the trait

466 space. Results showed similar trends for all the combinations of traits and number of
467 species used in the analyses (Figures D2, D3).

468

469 Importantly, compared to the other methods, the KIM methods sometimes generated a
470 different ranking between archipelagos for Jaccard dissimilarity. This is especially true for
471 woody species, for which KIM V3 suggests that trait turnover was higher for the Gambier
472 than for any other archipelagos, for all combinations of traits, and for both Jaccard and
473 Williams replacement indices (Figures 9, D2, D3). By contrast, the other methods generated
474 results that were more variable depending on the combination of traits and species used.

475

476 Randomisation of presence-absence matrices show that the KDH V2, KIM V2, KIM V3 and
477 Tree methods tended to generate more consistent values for Jaccard dissimilarity compared
478 to the convex hull, KDH V1 and KIM V1 methods (Figure D4). For Williams replacement,
479 values were also more consistent across randomised matrices for KIM V3 than for the other
480 methods, especially for herbaceous species.

481

482 4. Discussion

483

484 Here we compared existing and novel methods to compute trait turnover for simulated and
485 empirical data, to illustrate how differences in the computational aspects of these methods
486 reflect different aspects of trait diversity and can affect inferences made from trait diversity
487 comparisons.

488

489 4.1. Theoretical aspects of trait turnover computation

490

491 Comparing the seven methods using simulated data, for which we had complete control of
492 the community trait profiles in the trait space, revealed the important effects of the
493 computational specifics of each method on the value of trait β diversity. In particular, we
494 assessed the effect of conserving trait distance between species by comparing the tree-
495 based method, which distorts the trait distance between species in the dendrogram (Maire
496 et al., 2015), to the trait space-based methods. The tree-based method consistently

497 generated results most different from theoretical expectations (Figures 5-8). It tended to
498 either underestimate or overestimate dissimilarity in the trait profiles of communities in the
499 MCPs, and tended to generate high values for the Williams replacement index.

500

501 Interestingly, the convex-hull methods produced results similar to the tree-based method
502 for Jaccard dissimilarity, also generating results that differed from theoretical expectations.
503 This is because CONVHULL only uses a subset of the species in the trait space. Although
504 using a trait space approach better conserves trait distance between species than a tree-
505 based approach when all species are included, this property is broken when species are
506 ignored in the computation of trait turnover. Therefore, although the CONVHULL and tree-
507 based methods have been contrasted in the literature and have been shown to generate
508 different results (e.g. Loiseau et al., 2017), we show that neither of these two methods
509 accurately reflects the trait profile of a community.

510

511 In contrast, the other five trait space methods compared in this article (KDH V1-V2 and KIM
512 V1-V3) generated results more in line with theoretical expectations. These methods
513 therefore offer a more consistent representation of the community trait profile in the trait
514 space, i.e. they better capture the contribution of all species to the assessment of turnover.
515 The computational aspects of these approaches to estimating trait turnover have
516 nonetheless important effects on the generated β values, with potential consequences for
517 inferences about made trait turnover in an assemblage or community.

518

519 Specifically, we explored three computational aspects of these methods: (i) the use of
520 polytopes vs kernel integrals (KDH V1 vs KIM V1; Eqs 1 & 2 vs Eqs 5 & 6); (ii) the use of the
521 same or different bandwidths for each community in a pair when computing the KDE (KDH
522 V1 vs V2 and KIM V1 vs V2); and (iii) the use of point resampling when computing the KDE
523 (KIM V2 vs V3). All three aspects proved to have important effects on the β diversity values
524 calculated. Using kernel integrals, the same bandwidth and not resampling (i.e. using KIM
525 V3) generated results most in line with theoretical expectations.

526

527 The respective effects of these three computational aspects on trait turnover (β values)
528 depend on the index used (Jaccard dissimilarity or Williams replacement) and on the

529 configuration of the community trait profiles. For example, Jaccard dissimilarity is sensitive
530 to the difference in bandwidth between communities (Figure 6). This is because using
531 different bandwidths changes the shape of the KDEs (akin to making the distributions larger
532 or narrower in Figure 3) and generates polytopes with different areas (akin to changing the
533 lengths of A and B in Figure 3). Consequently, Jaccard dissimilarity values reflect this
534 artificial difference in trait richness, but not by Williams replacement. In contrast, for
535 Williams replacement, the use of polytopes or kernel integrals proved to be the most
536 important factor (Figure 7). This is because kernel integrals better reflect small variations in
537 the shape of the KDE (akin to changing the shape of the distributions and the overlapping
538 area in Figure 3) and thus better capture trait replacement. Similarly, resampling also
539 affected Williams replacement for communities with an “overlapping” configuration (Figure
540 7), especially for species-poor communities. This is because, when compared to the more
541 uniformly distributed trait profile of species-rich communities, each species has a greater
542 weight on the shape of the trait profile in species-poor communities, and the idiosyncrasy in
543 the position of different species can drastically change trait profiles if resampling is not
544 applied.

545

546 Both trait envelope, as captured by a convex hull, and kernel-based community trait profiles
547 have complementary uses, and the choice of an analytical approach will depend on the
548 research or management question. On the one hand, species with extreme trait values
549 defining a trait envelope for a given community can help capture the whole range of trait
550 values of species that may potentially join the community. The trait envelope may therefore
551 be an important piece of information to assess the risk of potential invaders to a region (
552 e.g. the join the locals vs. the try harder hypothesis; Tecco et al., 2010), or an indicator of
553 the loss of trait extremes. The CONVHULL method is appropriate for such applications. On
554 the other hand, capturing the trait distribution of all species in a community in the trait
555 space provides a more comprehensive description of trait diversity and is necessary for
556 identifying community assembly processes (Falster et al., 2017). The distributional profile of
557 species in the trait space can also highlight gaps within the trait envelope, where introduced
558 species with corresponding traits could have a higher chance to establish (i.e. the “empty
559 niche hypothesis”; MacArthur, 1970; Molofsky et al., 2022). This community trait profile
560 thus reflects ecosystem resilience and trait redundancy (Hui et al., 2021; Mouillot et al.,

561 2021). Our results suggest that the KIM V3 method is most informative and least biased for
562 addressing trait diversity questions.

563

564 4.2. Empirical test of methods using plant data from French Polynesia

565

566 The empirical testing of these methods provided further insight on the behaviour of the
567 different methods for a mixture of configurations of species points in the trait space (Figure
568 D1), and on how using different indices can lead to different conclusions. The KIM V3
569 method consistently generated much higher values for the contribution of replacement to
570 turnover than other methods, even when randomising site-by-species matrices (Figures 9,
571 D2-D4), suggesting that the higher Jaccard dissimilarity values generated by the other
572 methods may reflect an overestimation of the contribution of trait richness difference (the
573 complement of replacement) to turnover. Importantly, depending on the method used, one
574 could either conclude that most islands of an archipelago are very different from each other
575 in terms of trait diversity (e.g. Jaccard dissimilarity values > 0.5 for KIM V1 for the Gambier,
576 Tuamotu and Society archipelagos), or very similar (Jaccard dissimilarity values mostly < 0.2
577 for KIM V3). These different conclusions, in addition to the different rankings generated by
578 the different methods could be crucial for conservation decisions. For example, assuming
579 management actions are influenced by species traits, low trait dissimilarity between islands,
580 as indicated by KIM V3, would suggest that a similar management approach is appropriate
581 across most islands, simplifying management and potentially improving management
582 efficiency. In addition, the high contribution of replacement to turnover suggests that
583 existing differences in community trait profiles are unlikely to be the result of differences in
584 colonisation pressure, and may point towards either idiosyncratic or niche-driven factors.

585

586 5. Final recommendations / Conclusion

587

588 The kernel integral method presented here computes trait β diversity by directly integrating
589 KDEs. Out of the three different indices this method can generate, KIM V3 implements the
590 same bandwidth for the paired communities without resampling random points to uniform
591 distribution. KIM V3 generates values that better reflect the distribution of species in the

592 trait space (i.e. the community trait profiles) than methods based on convex hulls or
593 dendrograms, and also better than other methods based on KDEs. The approach is also
594 flexible, information rich and readily adapted to account for relative abundance between
595 species and intraspecific trait variation, by using different numbers of random points and
596 radii to generate the KDEs. Together with the convex hull method to inform on the trait
597 envelope, and tree-based approaches for quantifying phylogenetic diversity, and the kernel
598 integral method using the same bandwidth and non-uniform point distribution provide a
599 complementary set of metrics for understanding patterns of trait diversity and turnover.

600

601

602 Acknowledgements

603 We thank Jean-Yves Meyer for his time and expertise to refine the database on naturalised
604 alien plants species in French Polynesian islands. CH is supported by the NRF (89967), the
605 NERC (NE/V007548/1) and the Horizon Europe (101059592).

606

607

608 References

609

610 Ackerly, D. D., & Cornwell, W. K. (2007). A trait-based approach to community assembly:

611 Partitioning of species trait values into within- and among-community components.

612 *Ecology Letters*, *10*(2), 135–145. <https://doi.org/10.1111/j.1461-0248.2006.01006.x>

613 Anderson, M. J., Crist, T. O., Chase, J. M., Vellend, M., Inouye, B. D., Freestone, A. L.,

614 Sanders, N. J., Cornell, H. V., Comita, L. S., & Davies, K. F. (2011). Navigating the

615 multiple meanings of β diversity: A roadmap for the practicing ecologist. *Ecology*

616 *Letters*, *14*(1), 19–28.

617 Baselga, A. (2010). Partitioning the turnover and nestedness components of beta diversity.

618 *Global Ecology and Biogeography*, *19*(1), 134–143.

619 Baselga, A., & Leprieur, F. (2015). Comparing methods to separate components of beta
620 diversity. *Methods in Ecology and Evolution*, 6(9), 1069–1079.
621 <https://doi.org/10.1111/2041-210X.12388>

622 Blonder, B., Morrow, C. B., Maitner, B., Harris, D. J., Lamanna, C., Violle, C., Enquist, B. J., &
623 Kerkhoff, A. J. (2018). New approaches for delineating n-dimensional hypervolumes.
624 *Methods in Ecology and Evolution*, 9(2), 305–319. [https://doi.org/10.1111/2041-](https://doi.org/10.1111/2041-210X.12865)
625 [210X.12865](https://doi.org/10.1111/2041-210X.12865)

626 Cadotte, M. W., Carscadden, K., & Mirotnick, N. (2011). Beyond species: Functional
627 diversity and the maintenance of ecological processes and services. *Journal of*
628 *Applied Ecology*, 48(5), 1079–1087. [https://doi.org/10.1111/j.1365-](https://doi.org/10.1111/j.1365-2664.2011.02048.x)
629 [2664.2011.02048.x](https://doi.org/10.1111/j.1365-2664.2011.02048.x)

630 Cardoso, P., Mammola, S., Rigal, F., & Carvalho, J. (2022). *BAT: Biodiversity Assessment*
631 *Tools. R package version 2.8.1*. <https://CRAN.R-project.org/package=BAT>

632 Cardoso, P., Rigal, F., & Carvalho, J. C. (2015). BAT – Biodiversity Assessment Tools, an R
633 package for the measurement and estimation of alpha and beta taxon, phylogenetic
634 and functional diversity. *Methods in Ecology and Evolution*, 6(2), 232–236.
635 <https://doi.org/10.1111/2041-210X.12310>

636 Cardoso, P., Rigal, F., Carvalho, J. C., Fortelius, M., Borges, P. A. V., Podani, J., & Schmera, D.
637 (2014). Partitioning taxon, phylogenetic and functional beta diversity into
638 replacement and richness difference components. *Journal of Biogeography*, 41(4),
639 749–761. <https://doi.org/10.1111/jbi.12239>

640 Carmona, C. P., Azcárate, F. M., de Bello, F., Ollero, H. S., Lepš, J., & Peco, B. (2012).
641 Taxonomical and functional diversity turnover in Mediterranean grasslands:

642 Interactions between grazing, habitat type and rainfall. *Journal of Applied Ecology*,
643 49(5), 1084–1093. <https://doi.org/10.1111/j.1365-2664.2012.02193.x>

644 Carvalho, J. C., Cardoso, P., Borges, P. A. V., Schmera, D., & Podani, J. (2013). Measuring
645 fractions of beta diversity and their relationships to nestedness: A theoretical and
646 empirical comparison of novel approaches. *Oikos*, 122(6), 825–834.
647 <https://doi.org/10.1111/j.1600-0706.2012.20980.x>

648 Carvalho, J. C., Cardoso, P., & Gomes, P. (2012). Determining the relative roles of species
649 replacement and species richness differences in generating beta-diversity patterns.
650 *Global Ecology and Biogeography*, 21(7), 760–771. [https://doi.org/10.1111/j.1466-](https://doi.org/10.1111/j.1466-8238.2011.00694.x)
651 8238.2011.00694.x

652 Chao, A., Chazdon, R. L., Colwell, R. K., & Shen, T.-J. (2005). A new statistical approach for
653 assessing similarity of species composition with incidence and abundance data.
654 *Ecology Letters*, 8(2), 148–159. <https://doi.org/10.1111/j.1461-0248.2004.00707.x>

655 Chao, A., Chiu, C.-H., Villéger, S., Sun, I.-F., Thorn, S., Lin, Y.-C., Chiang, J.-M., & Sherwin, W.
656 B. (2019). An attribute-diversity approach to functional diversity, functional beta
657 diversity, and related (dis)similarity measures. *Ecological Monographs*, 89(2),
658 e01343. <https://doi.org/10.1002/ecm.1343>

659 Cornwell, W. K., Schwillk, D. W., & Ackerly, D. D. (2006). A trait-based test for habitat
660 filtering: Convex hull volume. *Ecology*, 87(6), 1465–1471.
661 [https://doi.org/10.1890/0012-9658\(2006\)87\[1465:ATTFHF\]2.0.CO;2](https://doi.org/10.1890/0012-9658(2006)87[1465:ATTFHF]2.0.CO;2)

662 Deane, D. C., Xing, D., Hui, C., McGeoch, M., & He, F. (2022). A null model for quantifying the
663 geometric effect of habitat subdivision on species diversity. *Global Ecology and*
664 *Biogeography*, 31(3), 440–453. <https://doi.org/10.1111/geb.13437>

665 Devictor, V., Mouillot, D., Meynard, C., Jiguet, F., Thuiller, W., & Mouquet, N. (2010). Spatial
666 mismatch and congruence between taxonomic, phylogenetic and functional
667 diversity: The need for integrative conservation strategies in a changing world.
668 *Ecology Letters*, 13(8), 1030–1040.

669 Díaz, S., Kattge, J., Cornelissen, J. H. C., Wright, I. J., Lavorel, S., Dray, S., Reu, B., Kleyer, M.,
670 Wirth, C., Colin Prentice, I., Garnier, E., Bönisch, G., Westoby, M., Poorter, H., Reich,
671 P. B., Moles, A. T., Dickie, J., Gillison, A. N., Zanne, A. E., ... Gorné, L. D. (2016). The
672 global spectrum of plant form and function. *Nature*, 529(7585), 167–171.
673 <https://doi.org/10.1038/nature16489>

674 Falster, D. S., Brännström, Å., Westoby, M., & Dieckmann, U. (2017). Multitrait successional
675 forest dynamics enable diverse competitive coexistence. *Proceedings of the National*
676 *Academy of Sciences*, 114(13), E2719–E2728.

677 Falster, D. S., Gallagher, R., Wenk, E. H., Wright, I. J., Indiarto, D., Andrew, S. C., Baxter, C.,
678 Lawson, J., Allen, S., Fuchs, A., Monro, A., Kar, F., Adams, M. A., Ahrens, C. W.,
679 Alfonzetti, M., Angevin, T., Apgaua, D. M. G., Arndt, S., Atkin, O. K., ... Ziemińska, K.
680 (2021). AusTraits, a curated plant trait database for the Australian flora. *Scientific*
681 *Data*, 8(1), 254. <https://doi.org/10.1038/s41597-021-01006-6>

682 Fitter, A. H., & Peat, H. J. (1994). The Ecological Flora Database. *Journal of Ecology*, 82(2),
683 415–425. JSTOR. <https://doi.org/10.2307/2261309>

684 Fourdrigniez, M., & Meyer, J.-Y. (2008). *Liste et caractéristiques des plantes introduites*
685 *naturalisées et envahissantes en Polynésie française* (No. 17; Contributions à La
686 Biodiversité de Polynésie Française). Délégation à la Recherche, Papeete, 64 pages.

687 Gotelli, N. J. (2000). NULL MODEL ANALYSIS OF SPECIES CO-OCCURRENCE PATTERNS.
688 *Ecology*, 81(9), 2606–2621. <https://doi.org/10.1890/0012->
689 9658(2000)081[2606:NMAOSC]2.0.CO;2

690 Gross, N., Bagousse-Pinguet, Y. L., Liancourt, P., Berdugo, M., Gotelli, N. J., & Maestre, F. T.
691 (2017). Functional trait diversity maximizes ecosystem multifunctionality. *Nature*
692 *Ecology & Evolution*, 1(5), 0132. <https://doi.org/10.1038/s41559-017-0132>

693 Hill, M. O., Preston, C. D., & Roy, D. B. (2004). *PLANTATT - Attributes of British and Irish*
694 *Plants—Spreadsheet*. Centre for Ecology and Hydrology.

695 Hillebrand, H., & Matthiessen, B. (2009). Biodiversity in a complex world: Consolidation and
696 progress in functional biodiversity research. *Ecology Letters*, 12(12), 1405–1419.
697 <https://doi.org/10.1111/j.1461-0248.2009.01388.x>

698 Hui, C., Richardson, D. M., Landi, P., Minoarivelo, H. O., Roy, H. E., Latombe, G., Jing, X.,
699 CaraDonna, P. J., Gravel, D., Beckage, B., & Molofsky, J. (2021). Trait positions for
700 elevated invasiveness in adaptive ecological networks. *Biological Invasions*, 23(6),
701 1965–1985. <https://doi.org/10.1007/s10530-021-02484-w>

702 Irl, S. D. H., Schweiger, A. H., Medina, F. M., Fernández-Palacios, J. M., Harter, D. E. V.,
703 Jentsch, A., Provenzale, A., Steinbauer, M. J., & Beierkuhnlein, C. (2017). An island
704 view of endemic rarity—Environmental drivers and consequences for nature
705 conservation. *Diversity and Distributions*, 23(10), 1132–1142.
706 <https://doi.org/10.1111/ddi.12605>

707 Jaccard, P. (1908). Nouvelles recherches sur la distribution florale. *Bull. Soc. Vaud. Sci. Nat.*,
708 44, 223–270.

709 Kattge, J., Bönisch, G., Díaz, S., Lavorel, S., Prentice, I. C., Leadley, P., Tautenhahn, S.,
710 Werner, G. D. A., Aakala, T., Abedi, M., Acosta, A. T. R., Adamidis, G. C., Adamson, K.,

711 Aiba, M., Albert, C. H., Alcántara, J. M., Alcázar C, C., Aleixo, I., Ali, H., ... Wirth, C.
712 (2020). TRY plant trait database – enhanced coverage and open access. *Global*
713 *Change Biology*, 26(1), 119–188. <https://doi.org/10.1111/gcb.14904>

714 Kattge, J., Díaz, S., Lavorel, S., Prentice, I. C., Leadley, P., Bönsch, G., Garnier, E., Westoby,
715 M., Reich, P. B., Wright, I. J., Cornelissen, J. H. C., Violle, C., Harrison, S. P., Van
716 Bodegom, P. M., Reichstein, M., Enquist, B. J., Soudzilovskaia, N. A., Ackerly, D. D.,
717 Anand, M., ... Wirth, C. (2011). TRY – a global database of plant traits. *Global Change*
718 *Biology*, 17(9), 2905–2935. <https://doi.org/10.1111/j.1365-2486.2011.02451.x>

719 Kleyer, M., Bekker, R. M., Knevel, I. C., Bakker, J. P., Thompson, K., Sonnenschein, M.,
720 Poschod, P., Van Groenendael, J. M., Klimeš, L., Klimešová, J., Klotz, S., Rusch, G. M.,
721 Hermy, M., Adriaens, D., Boedeltje, G., Bossuyt, B., Dannemann, A., Endels, P.,
722 Götzenberger, L., ... Peco, B. (2008). The LEDA Traitbase: A database of life-history
723 traits of the Northwest European flora. *Journal of Ecology*, 96(6), 1266–1274.
724 <https://doi.org/10.1111/j.1365-2745.2008.01430.x>

725 Kunin, W. E., Harte, J., He, F., Hui, C., Jobe, R. T., Ostling, A., Polce, C., Šizling, A., Smith, A. B.,
726 Smith, K., Storch, D., Even, T., Karl-Inne, U., Werner, U., & Varun, V. (2018). Upscaling
727 biodiversity: Estimating the species–area relationship from small samples. *Ecological*
728 *Monographs*, 88, 170–187.

729 Laureto, L. M. O., Cianciaruso, M. V., & Samia, D. S. M. (2015). Functional diversity: An
730 overview of its history and applicability. *Natureza & Conservação*, 13(2), 112–116.
731 <https://doi.org/10.1016/j.ncon.2015.11.001>

732 Loiseau, N., Legras, G., Gaertner, J., Verley, P., Chabanet, P., & Mérigot, B. (2017).
733 Performance of partitioning functional beta-diversity indices: Influence of functional

734 representation and partitioning methods. *Global Ecology and Biogeography*, 26(6),
735 753–762.

736 MacArthur, R. (1970). Species packing and competitive equilibrium for many species.
737 *Theoretical Population Biology*, 1(1), 1–11.

738 Maire, E., Grenouillet, G., Brosse, S., & Villéger, S. (2015). How many dimensions are needed
739 to accurately assess functional diversity? A pragmatic approach for assessing the
740 quality of functional spaces. *Global Ecology and Biogeography*, 24(6), 728–740.
741 <https://doi.org/10.1111/geb.12299>

742 Maitner, B. (2022). *BIEN: Tools for Accessing the Botanical Information and Ecology Network*
743 *Database. R package version 1.2.5.* <https://CRAN.R-project.org/package=BIEN>

744 Mammola, S., & Cardoso, P. (2020). Functional diversity metrics using kernel density n-
745 dimensional hypervolumes. *Methods in Ecology and Evolution*, 11(8), 986–995.
746 <https://doi.org/10.1111/2041-210X.13424>

747 McGill, B. J., Enquist, B. J., Weiher, E., & Westoby, M. (2006). Rebuilding community ecology
748 from functional traits. *Trends in Ecology & Evolution*, 21(4), 178–185.

749 Middleton-Welling, J., Dapporto, L., García-Barros, E., Wiemers, M., Nowicki, P., Plazio, E.,
750 Bonelli, S., Zaccagno, M., Šašić, M., Liparova, J., Schweiger, O., Harpke, A., Musche,
751 M., Settele, J., Schmucki, R., & Shreeve, T. (2020). A new comprehensive trait
752 database of European and Maghreb butterflies, Papilionoidea. *Scientific Data*, 7(1),
753 351. <https://doi.org/10.1038/s41597-020-00697-7>

754 Molofsky, J., Park, D. S., Richardson, D. M., Keller, S. R., Beckage, B., Mandel, J. R.,
755 Boatwright, J. S., & Hui, C. (2022). Optimal differentiation to the edge of trait space
756 (EoTS). *Evolutionary Ecology*, 36(5), 743–752. [https://doi.org/10.1007/s10682-022-](https://doi.org/10.1007/s10682-022-10192-7)
757 10192-7

758 Mouillot, D., Loiseau, N., Grenié, M., Algar, A. C., Allegra, M., Cadotte, M. W., Casajus, N.,
759 Denelle, P., Guéguen, M., Maire, A., Maitner, B., McGill, B. J., McLean, M., Mouquet,
760 N., Munoz, F., Thuiller, W., Villéger, S., Violle, C., & Auber, A. (2021). The
761 dimensionality and structure of species trait spaces. *Ecology Letters*, *24*(9), 1988–
762 2009. <https://doi.org/10.1111/ele.13778>

763 Mouillot, D., Stubbs, W., Faure, M., Dumay, O., Tomasini, J. A., Wilson, J. B., & Chi, T. D.
764 (2005). Niche overlap estimates based on quantitative functional traits: A new family
765 of non-parametric indices. *Oecologia*, *145*(3), 345–353.
766 <https://doi.org/10.1007/s00442-005-0151-z>

767 Petchey, O. L., & Gaston, K. J. (2006). Functional diversity: Back to basics and looking
768 forward. *Ecology Letters*, *9*(6), 741–758. [https://doi.org/10.1111/j.1461-](https://doi.org/10.1111/j.1461-0248.2006.00924.x)
769 [0248.2006.00924.x](https://doi.org/10.1111/j.1461-0248.2006.00924.x)

770 R Core Team. (2022). *R: A language and environment for statistical computing*. R Foundation
771 *for Statistical Computing, Vienna, Austria*. <https://www.R-project.org/>

772 Siefert, A., Ravenscroft, C., Weiser, M. D., & Swenson, N. G. (2013). Functional beta-diversity
773 patterns reveal deterministic community assembly processes in eastern North
774 American trees. *Global Ecology and Biogeography*, *22*(6), 682–691.
775 <https://doi.org/10.1111/geb.12030>

776 Sobral, F. L., Lees, A. C., & Cianciaruso, M. V. (2016). Introductions do not compensate for
777 functional and phylogenetic losses following extinctions in insular bird assemblages.
778 *Ecology Letters*, *19*(9), 1091–1100. <https://doi.org/10.1111/ele.12646>

779 Socolar, J. B., Gilroy, J. J., Kunin, W. E., & Edwards, D. P. (2016). How should beta-diversity
780 inform biodiversity conservation? *Trends in Ecology & Evolution*, *31*(1), 67–80.

781 Swenson, N. G., Erickson, D. L., Mi, X., Bourg, N. A., Forero-Montaña, J., Ge, X., Howe, R.,
782 Lake, J. K., Liu, X., Ma, K., Pei, N., Thompson, J., Uriarte, M., Wolf, A., Wright, S. J., Ye,
783 W., Zhang, J., Zimmerman, J. K., & Kress, W. J. (2012). Phylogenetic and functional
784 alpha and beta diversity in temperate and tropical tree communities. *Ecology*,
785 *93*(sp8), S112–S125. <https://doi.org/10.1890/11-0402.1>

786 Tavşanoğlu, Ç., & Pausas, J. G. (2018). A functional trait database for Mediterranean Basin
787 plants. *Scientific Data*, *5*(1), 180135. <https://doi.org/10.1038/sdata.2018.135>

788 Tecco, P. A., Díaz, S., Cabido, M., & Urcelay, C. (2010). Functional traits of alien plants across
789 contrasting climatic and land-use regimes: Do aliens join the locals or try harder than
790 them? *Journal of Ecology*, *98*(1), 17–27.

791 Tobias, J. A., Sheard, C., Pigot, A. L., Devenish, A. J. M., Yang, J., Sayol, F., Neate-Clegg, M. H.
792 C., Alioravainen, N., Weeks, T. L., Barber, R. A., Walkden, P. A., MacGregor, H. E. A.,
793 Jones, S. E. I., Vincent, C., Phillips, A. G., Marples, N. M., Montaña-Centellas, F. A.,
794 Leandro-Silva, V., Claramunt, S., ... Schleuning, M. (2022). AVONET: morphological,
795 ecological and geographical data for all birds. *Ecology Letters*, *25*(3), 581–597.
796 <https://doi.org/10.1111/ele.13898>

797 Villéger, S., Grenouillet, G., & Brosse, S. (2013). Decomposing functional β -diversity reveals
798 that low functional β -diversity is driven by low functional turnover in European fish
799 assemblages. *Global Ecology and Biogeography*, *22*(6), 671–681.
800 <https://doi.org/10.1111/geb.12021>

801 Villéger, S., Maire, E., & Leprieux, F. (2017). On the risks of using dendrograms to measure
802 functional diversity and multidimensional spaces to measure phylogenetic diversity:
803 A comment on Sobral et al. (2016). *Ecology Letters*, *20*(4), 554–557.
804 <https://doi.org/10.1111/ele.12750>

805 Villéger, S., Mason, N. W. H., & Mouillot, D. (2008). New multidimensional functional
806 diversity indices for a multifaceted framework in functional ecology. *Ecology*, *89*(8),
807 2290–2301. <https://doi.org/10.1890/07-1206.1>

808 Westoby, M. (1998). A leaf-height-seed (LHS) plant ecology strategy scheme. *Plant and Soil*,
809 *199*(2), 213–227. <https://doi.org/10.1023/A:1004327224729>

810 Williams, P. H. (1996). Mapping variations in the strength and breadth of biogeographic
811 transition zones using species turnover. *Proceedings of the Royal Society B: Biological*
812 *Sciences*, *263*(1370), 579–588. <https://doi.org/10.1098/rspb.1996.0087>

813 Wohlwend, M. R., Craven, D., Weigelt, P., Seebens, H., Winter, M., Kreft, H., Dawson, W.,
814 Essl, F., van Kleunen, M., & Pergl, J. (2021). Data descriptor: Pacific introduced flora
815 (PaciFLora). *Biodiversity Data Journal*, *9*.

816

817 **Tables**

818

819 **Table 1.** Summary of the methods used to compute trait turnover.

Method	Summary	Advantages	Caveats	References
Convex hull method (COVHULL)	A minimum convex polytope (MCP) encompassing all species points in the trait space is computed for each community. The hypervolumes are used in the computation of the β diversity indices.	The distance between the original species points in the trait space is representative of how functionally different the species are.	Only the species with extreme trait values are used in the computation of the β diversity indices. Sensitive to outliers.	(Cornwell et al., 2006; Villéger et al., 2008, 2013)
Tree-based method (TREE)	A dendrogram is computed for the species pool based on the distance between all species based on their traits. The resulting tree is trimmed for each community, and the lengths of branches are used in the computation of the β diversity indices.	All species contribute to the computation of the β diversity indices. Not as sensitive to outliers as the convex hull method.	The distance between the species computed from the dendrograms is somewhat different from the original trait difference between species for the traits considered in the analyses.	(Cardoso et al., 2014)
Kernel density hypervolume (KDH) V1	A polytope is computed for each community based on a kernel density estimator (KDE). The hypervolumes are used in the computation of the β diversity indices.	The distance between the original species points in the trait space is representative of how functionally different the species are. The polytope accounts for how species are distributed in the trait space.	Sensitive to the threshold used to compute the MCP. The random points are resampled to uniform distribution, which diminishes the effect of the species point distributions in the trait space. A different bandwidth is used for each community to generate the random points and compute the KDE. As a result, the KDE is influenced by the distance between the species in the trait space.	(Mammola & Cardoso, 2020)

Kernel density hypervolume (KDH) V2	As KDH V1, but using the same bandwidth for each pair of communities.	As KDH V1, plus independence from how different species are from each other in each community.	As KDH V1, except for the issue related to using different bandwidths.	This article
Kernel Integral Method (KIM) V1	The β diversity indices are directly computed from KDEs of species points in the trait space. The KDEs are based on the same procedure as KDH V1.	As KDH V1, but with the advantage of being insensitive to the threshold used to compute the MCP.		This article
Kernel Integral Method (KIM) V2	As KIM V1, but using the same bandwidth for each pair of communities.	As KDH V2, but with the advantage of being insensitive to the threshold used to compute the MCP.		This article
Kernel Integral Method (KIM) V3	The β diversity indices are directly computed from kernel density estimators of species points in the trait space, but the KDEs are estimated directly from points randomly drawn around species points in the trait space, without resampling to uniform density.	As KDH V1 & V2, but reflecting more accurately the distribution of species points in the trait space. The radius of the hyperspheres still needs to be determined.		This article

820

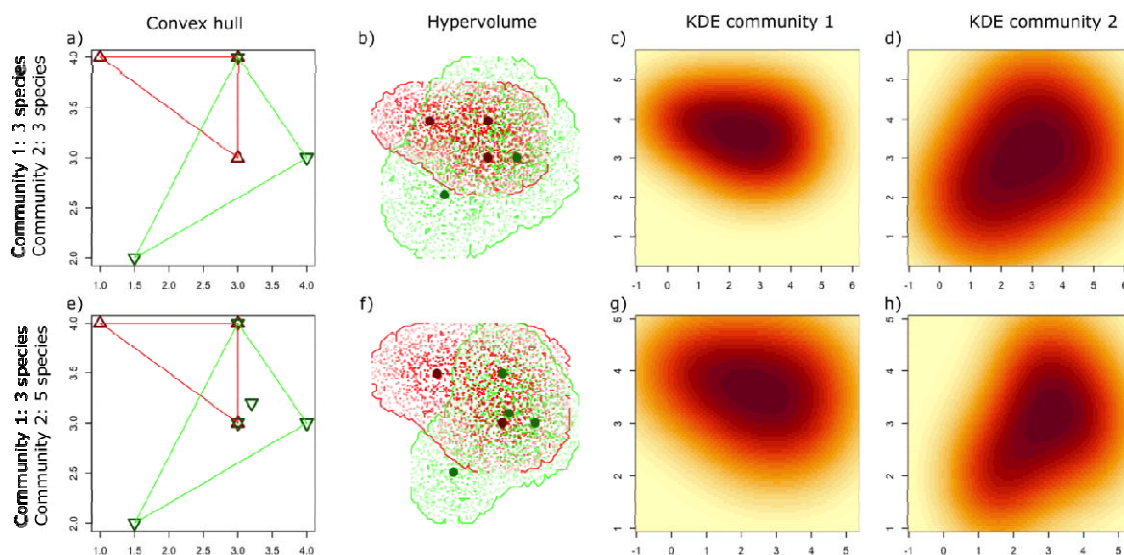
821

822 **Figures**

823

824

825



826

827

828

829

830

831

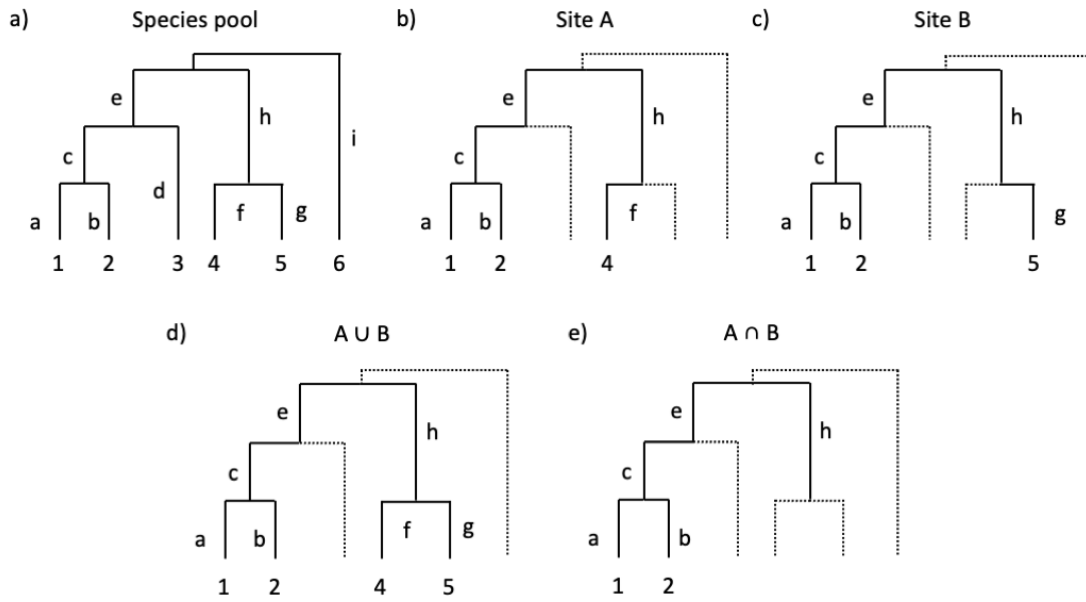
832

833

834

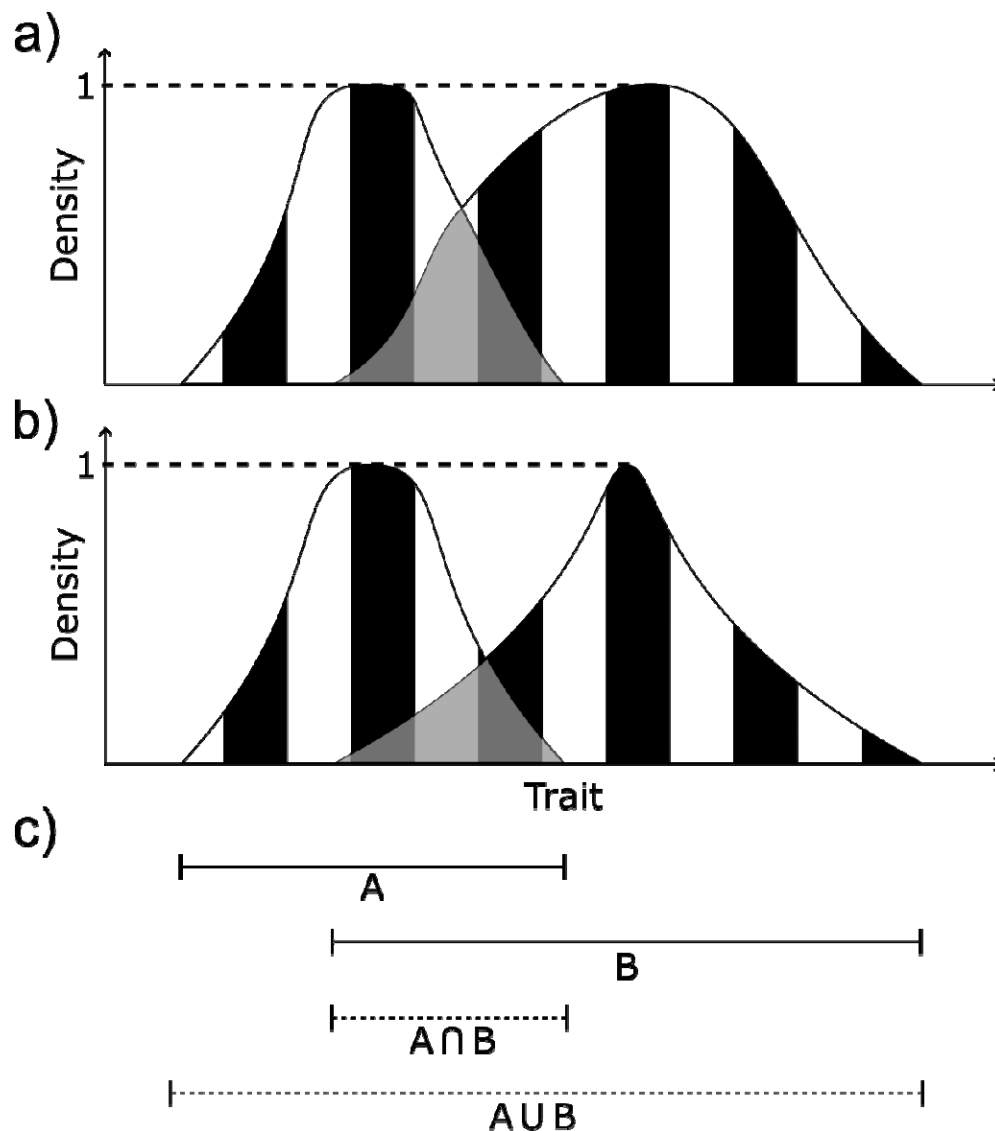
835

Figure 1. Summary of the trait space approaches for two communities with different species in a two-dimensional trait space. a,e) The convex hull remains the same irrespective of the additional species present in community 2, resulting in the same outcome when computing β diversity metrics. b,f) The KDH (kernel density hypervolume) method generates a polytope for each community, whose shape will vary with the absence or presence of the additional species in community 2 and is often non-convex. As a result, the outcome of the Jaccard dissimilarity or the Williams replacement formulas will differ. c,d) KDEs corresponding to the polytopes in (b). g,h) KDEs corresponding to the polytopes in (f).



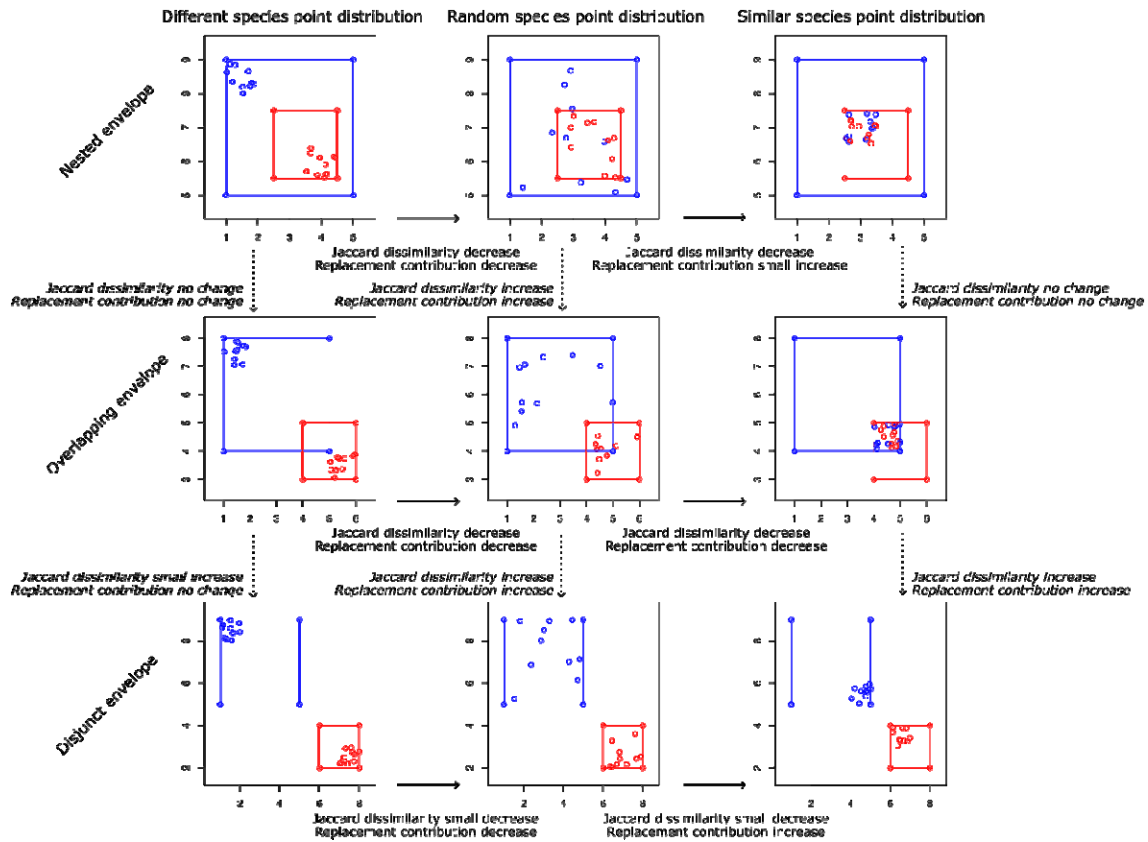
836
837
838
839
840
841
842
843
844
845

Figure 2. Components of the tree-based approach for the computation of trait turnover between two sites whose species are part of a larger species pool. a) Dendrogram for all species in the species pool. b) Dendrogram for species present in site A, after trimming the global tree from a). c) Dendrogram for species present in site B. d) Dendrogram for species present in either site A or site B. Since species 3 does not occur at any of the two sites, branch d is not included. e) Dendrogram for species present in both sites A and B. Although species 4 and 5 are present in only one of the two sites, branch h appears in both dendrograms, and is therefore conserved.



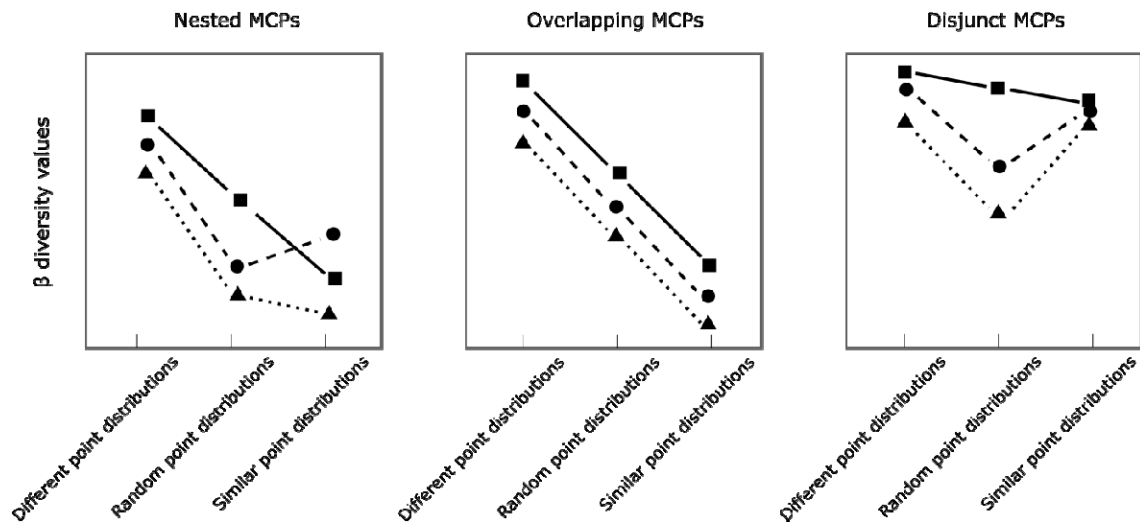
846
 847
 848
 849
 850
 851
 852
 853
 854
 855
 856
 857
 858
 859
 860

Figure 3. Details of the computation of trait turnover for two pairs of communities (one pair in (a) and one in (b)) following different approaches. In each graph (a,b), the curves fictional KDEs (Kernel density estimators) for the two communities, in one dimension (for simplification, we assume their densities are 0 beyond intersecting the horizontal axis). Using the KIM (Kernel integration method) formula, The Jaccard index is computed as one minus the area in grey divided by the striped area (Eq. 5), and the value is different for the two pairs of communities in (a) and (b) (as is the value of Willams replacement index, Eq. 6). (c) The horizontal segments represent one-dimensional polytopes (defined using the values where the KDEs intersect the horizontal axis for simplification), used to compute the Jaccard or Williams indices using the KDH (kernel density hypervolume) method (Eqs 1, 2). Contrary to KIM, the KDH method only generates a single value for each index for the two pairs of communities.



861
 862
 863
 864
 865
 866
 867
 868
 869
 870
 871

Figure 4. One of the 50 instances of the nine theoretical configurations of pairs of communities for different sizes of the MCPs (see Figure A1 for same size MCPs), using only 10 randomly drawn species points for clarity (point distributions for 40, 70 and 100 species were also generated). We varied how the MCPs overlapped (“nested”, “overlapping” or “disjunct”), and how the species points are distributed within the MCPs (“different” – distributed in opposite corners of the MCPs –, “random” – randomly distributed within the MCPs – or “similar” – distributed either within the same small area, or in the closest corners of the MCPs).



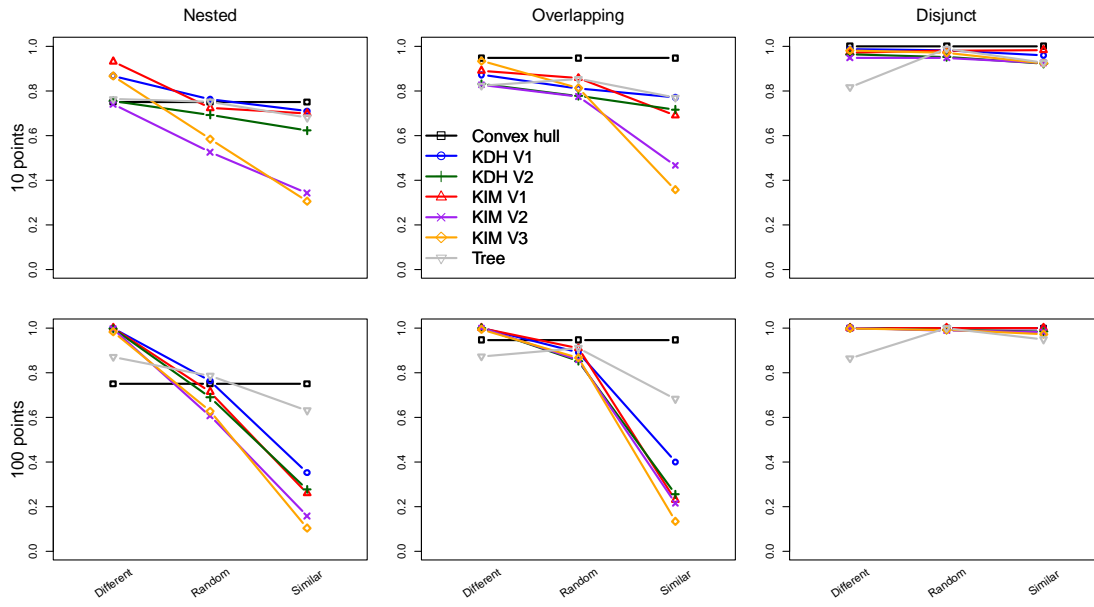
873

874

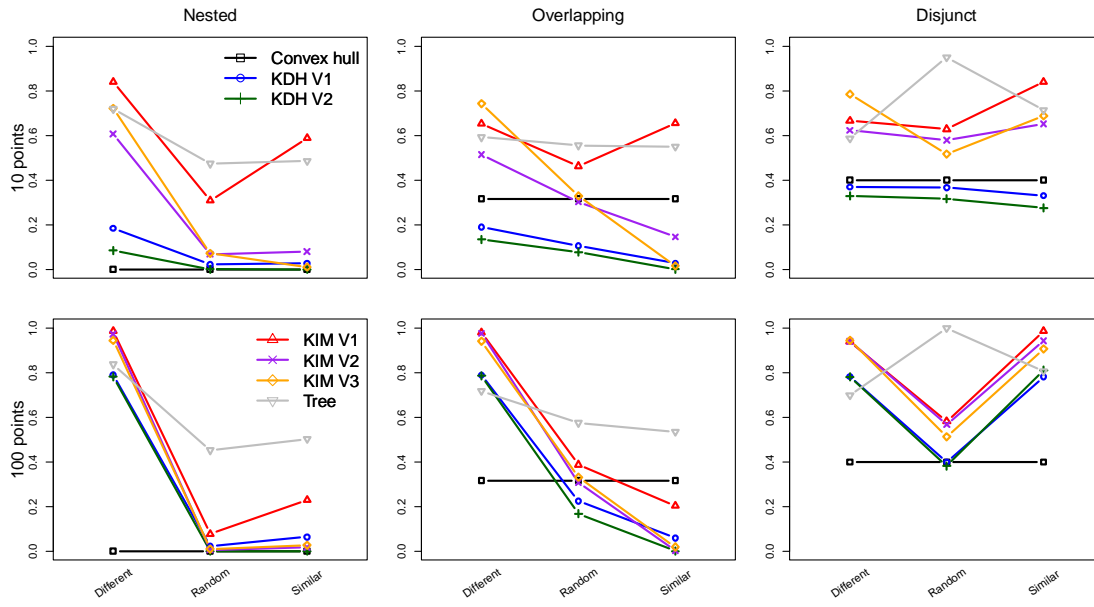
875 **Figure 5.** Qualitative differences in β values for trait turnover predicted under different
 876 simulated configurations of species points in the trait space when the MCPs of the two
 877 communities have different sizes. Jaccard dissimilarity (squares, solid lines), Williams
 878 replacement (triangles, dotted lines), and contribution of replacement to overall turnover,
 879 computed as Williams replacement divided by Jaccard dissimilarity (circles, dashed lines).
 880 Overall, β values, are expected to decrease as the overlap between the trait profiles of the
 881 two simulated communities increases. Jaccard dissimilarity accounts for differences in the
 882 spread of the trait profiles in the trait space (i.e. trait richness), whereas Williams
 883 replacement is independent from differences in trait richness. For detailed explanations
 884 about the changes in β values, see Table A1 in SI.

885

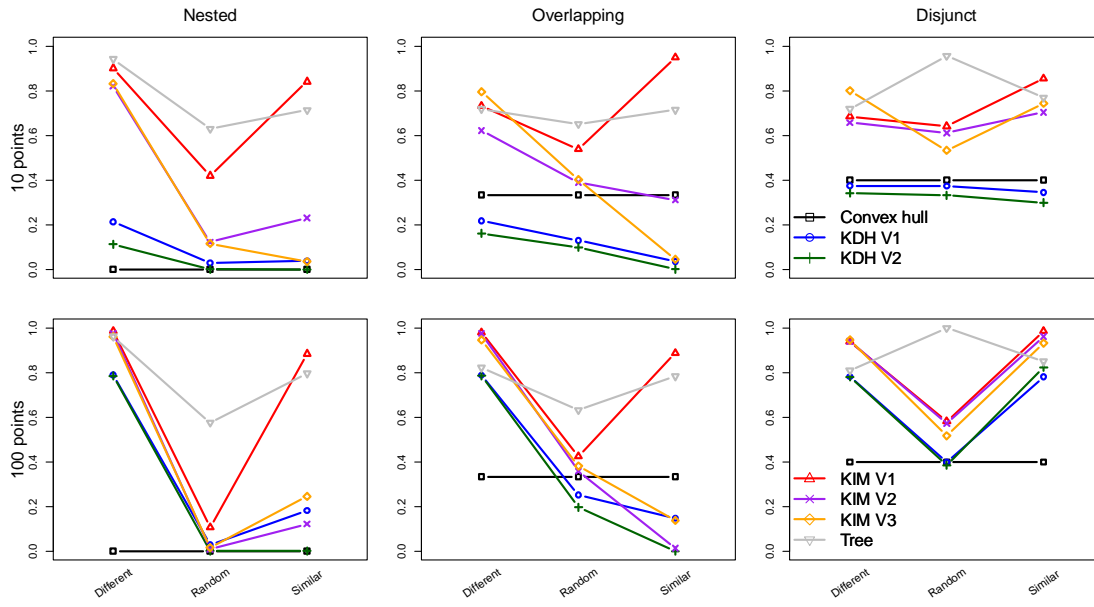
886



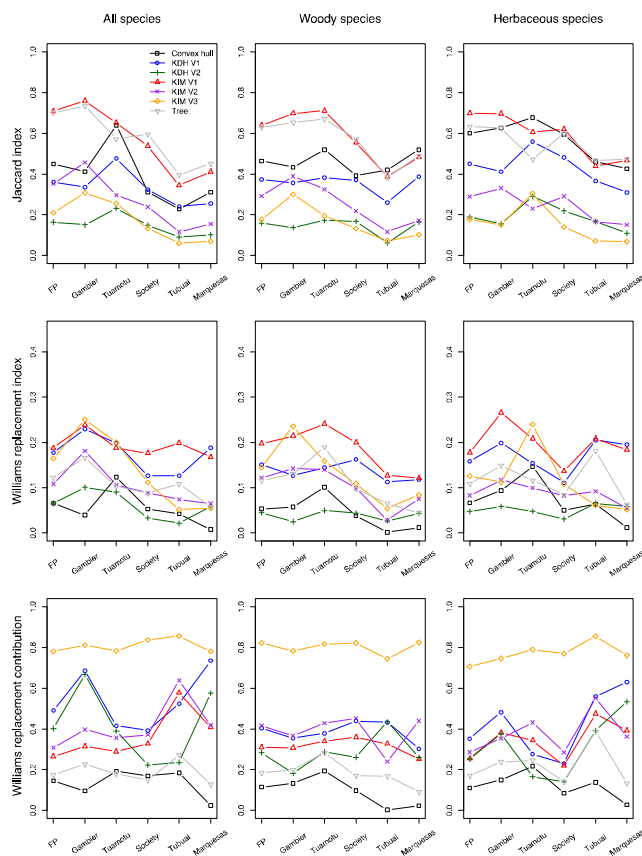
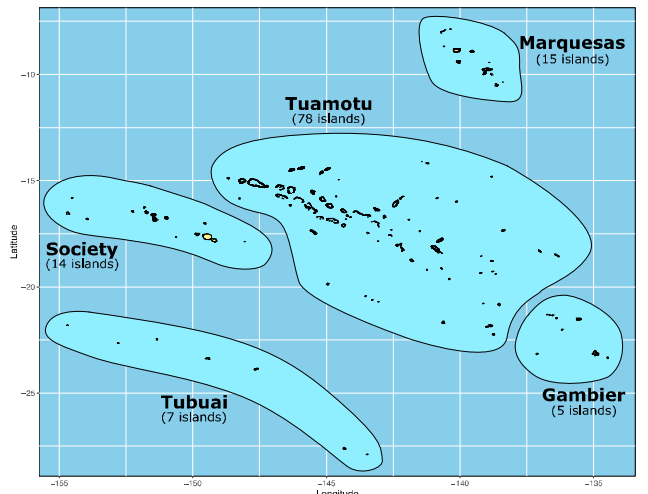
887
 888 **Figure 6.** Differences in Jaccard dissimilarity between the seven methods summarised in
 889 Table 1, for MCPs of different sizes, for 10 and 100 species points (see Appendix C for the
 890 full set of results).
 891



892
 893 **Figure 7.** Changes in Williams replacement index for the seven methods summarised in
 894 Table 1, for MCPs of different sizes, for 10 and 100 species points (see Appendix C for the
 895 full set of results).
 896



897
 898 **Figure 8.** Changes in the contribution of replacement to overall turnover, computed as
 899 Williams replacement divided by Jaccard dissimilarity, for the seven methods summarised in
 900 Table 1, for MCPs of different sizes (see Appendix C for the full set of results).
 901



902
903

904 **Figure 9.** Application of seven trait turnover methods to empirical data on French
905 Polynesian plant species. Jaccard dissimilarity index, Williams replacement index, and
906 contribution of replacement to overall turnover, computed as Williams replacement divided
907 by Jaccard dissimilarity, for the seven methods summarised in Table 1, for French Polynesia
908 (FP) and its archipelagos, for all species, woody species and herbaceous species, using seed
909 mass and plant height, for 250 out of 417 species (see Figures C2 and C3 for using seed
910 mass, plant height and SLA on 124 species, and seed mass and plant height on 124 species).
911 Note that the order of the islands is arbitrary, and lines between symbols are used as a
912 visual aid and not to depict continuous change.